# Heavy Oil Hydrocarbons and Kerogen Destruction of Carbonate–Siliceous Domanic Shale Rock in Sub- and Supercritical Water

**Zukhra R. Nasyrova** [1] , **Galina P. Kayukova** [2] , **Alexey V. Vakhin** [1,*] , **Richard Djimasbe** [1] and **Artem E. Chemodanov** [1]

[1]  Institute of Geology and Oil and Gas Technologies, Kazan Federal University, 18 Kremlyovskaya str., 420008 Kazan, Russia; nzr95@yandex.ru (Z.R.N.); oilchad91@gmal.com (R.D.); chemodanov41659@mail.ru (A.E.C.)

[2]  Arbuzov Institute of Organic and Physical Chemistry, FRC Kazan Scientific Center, Russian Academy of Sciences, 8 Akademika Arbuzova, 420088 Kazan, Russia; kayukova@iopc.ru

\*  Correspondence: vahin-a_v@mail.ru

**Abstract:** This paper discusses the results of the influences of subcritical (T = 320 °C; P = 17 MPa) and supercritical water (T = 374 °C; P = 24.6 MPa) on the yield and composition of oil hydrocarbons generated from carbonaceous–siliceous Domanic shale rocks with total organic content ($C_{org}$) of 7.07%. It was revealed that the treatment of the given shale rock in sub- and supercritical water environments resulted in the decrease of oil content due to the intensive gas formation. The content of light hydrocarbon fractions (saturated and aromatic hydrocarbons) increased at 320 °C from 33.98 to 39.63%, while at 374 °C to 48.24%. Moreover, the content of resins decreased by almost twice. Insoluble coke-like compounds such as carbene–carboids were formed due to decomposition of kerogen after supercritical water treatment. Analysis of oil hydrocarbons with FTIR method revealed a significant number of oxygen-containing compounds, which are the hydrogenolysis products of structural fragments formed after destruction of kerogen and high-molecular components of oil. The gas chromatography–mass spectroscopy (GC–MS) method was applied to present the changes in the composition of mono- and dibenzothiophenes, which indicate conversion of heavy components into lighter aromatic hydrocarbons. The specific features of transforming trace elements in rock samples, asphaltenes, and carbene–carboids were observed by using the isotopic mass-spectrometry method.

**Keywords:** heavy oil; kerogen; sub- and supercritical water; Domanic rock; shale; heavy hydrocarbons; organic matter

## 1. Introduction

In recent years, the share of unconventional hydrocarbon resources from shale deposits in the structure of world oil production has been increasing [1–3]. Low-permeable organic-rich Bazhen formations of West Siberia and Domanic deposits of Volga–Ural petroleum province correspond to such resources in Russia [4,5]. Domanic organic-rich shales are oil-generating source rocks [6]. A specific feature of such sedimentary rocks is the coexistence of free hydrocarbons and insoluble organic matter (OM), such as kerogen. The latter is an irregular structured "geopolymer" that generates oil and contains significant total organic content in sedimentary rocks [7,8]. The obtained experiences from the study of shale rocks in the USA show that Eagle Ford Shale Play in Mexican borders is the analogue of Sargaevskian–Tournaisian carbon-rich Domanic shale rock in Tatarstan Republic (Russia) in terms of geochemical characteristics [9]. Currently, Domanic sediments have been studied only

at the laboratory scale [10–13]. However, it is crucial to develop the production technology of such hydrocarbon resources in field scale.

Superheated organic solvents have been effectively applied in thermal cracking and chemical conversion of a wide range of high-molecular organic matter into volatile and soluble substances [14]. In recent years, there has been considerable interest in supercritical water (SCW) that accelerates thermochemical decomposition of fossil fuels [15,16]. Relative dielectric permittivity (e) of SCW varies between 2 and 30, depending on the pressure and temperature. Thereby, SCW may behave like favorable nonpolar hexane solvent (e = 1.8) or even like polar methanol solvent (e = 32.6) with high solubility for OM [17]. However, SCW is not only able to dissolve hydrocarbons, but it can also react with OM, its destruction products, and with rock minerals [18–20]. Due to these unique properties, supercritical fluid extraction attracted much attention by many scholars and researchers [21–24].

There are many studies which deal with the conversion of heavy oils and vacuum residues in subcritical water (sub-CW) and SCW conditions. Caniaz et al. [25] studied refinery of bitumen and domestic unconventional heavy oil upgrading in SCW. They made conclusions that SCW forms layers between asphaltenes, preventing their agglomeration and slowing down the formation of coke in the conversion products. Similar conclusions were made by researchers from Imperial College London regarding heavy oil upgrading in sub-CW and SCW [26]. They identified the effect of sub-CW and SCW on the conversion of modeled polyaromatic hydrocarbons that exist in asphaltenes and other heavy oil fractions. It has been established that SCW acts mainly on central rings of polyaromatic structures, rather than peripheral ones, initiating cracking reactions. In Reference [27], the authors investigated the transformation of vacuum residue fraction in SCW at 450 °C and established a double increase in the yield of valuable gasoline and diesel fractions and a significant decrease in the coke yield, in comparison with traditional refining methods. The cracking of the vacuum residue occurs with the intensive formation of hydrocarbon gases, light aliphatic hydrocarbons, alkylbenzenes, and alkylnaphthalenes. Other researchers studied the conversion of vacuum residue in SCW medium in order to obtain light oil [28]. Studies have shown that the most favorable condition for the use of SCW in the cracking of heavy hydrocarbons is at a temperature of 420 °C, a water density of 0.15 g/cm$^3$, a water–oil ratio of 2:1, and a reaction time of 1 h.

In the scientific literature, there are several works on the influence of sub-CW and SCW on the conversion of kerogen into light petroleum hydrocarbons, as well as their extraction. The hydrocarbon extraction from shale rock samples and Turkish lignite showed that SCW is the most effective method for conversion of asphaltenes and kerogen [29]. Water in supercritical state is able to penetrate the kerogen and heavy oil hydrocarbons structure and break their structural skeleton, leading to the formation of light petroleum hydrocarbons. Raising reaction temperature and pressure, or increasing reaction duration, results in more intensive decomposition of kerogen and heavy hydrocarbons. Funazukuri et al. [15] studied supercritical extraction of Chinese shale oil and observed that decomposition of polar components in SCW was more favorable than in supercritical toluene. A similar comparison of SCW and supercritical toluene was carried out by Olukcu et al. [30]. They state that the conversion degree due to transformation of Beypazari oil shale in SCW was higher than in supercritical toluene. Moreover, the content of asphaltenes and polar substances was higher in the oil after supercritical toluene treatment, in contrast to the oil after SCW treatment.

In general, an analysis of the current research in the field of heavy oil and kerogen conversion in sub-CW and SCW shows good prospects for this method as an alternative way to improve the quality of heavy hydrocarbons and the efficient petroleum hydrocarbons extraction from dense low-permeability Dominic rocks.

The aim of this study was to reveal the transformation behaviors of high-molecular components of heavy oil and insoluble kerogen from carbon-rich low-permeable carbonaceous–siliceous Domanic shale rocks in sub- and supercritical water.

## 2. Experimental Procedures

The object of the study was the Domanic rock, which was taken from 1720 m depth of the Semiluki-Mendym horizon of the Chishminskaya area, which is located on the largest Romashkino field territory (Tatarstan, Russia). The given rocks are characterized by the following mineral composition: 43% quartz, 19% calcite, 19% microcline, 12% mica, and 6% dolomite [31]. According to the data obtained by using the Rock-Eval pyrolysis method, the total organic content ($C_{org}$) in the rock sample is 7.07%. It shows that the content of free light hydrocarbons in the given rock sample is very low, and a significant part of OM corresponds to heavy components and insoluble kerogen [32].

The process was carried out by using a 500 mL high-pressure reactor with a stirrer—Parr Instruments 4560 (Parr Instruments, USA)—for 60 min. The processes in reactor were carried out at sub-CW at 320 °C and 17 MPa and SCW at 374 °C and 24.6 MPa. To achieve a water density that ensures the transition of water to a sub- and supercritical state at the experimental temperatures, the initial nitrogen pressure and the volume of required water were selected in accordance with the reference data of the National Institute of Standards and Technology [33]. In total, 100 g of crushed rock and 130 mL of distilled water were introduced into the reactor, for each experiment. The reactor was purged with nitrogen for 15 min before starting each experiment, and the given initial pressure was 1 MPa. The heating rate was 11 °C/min.

After cooling the reactor up to 25 °C, the reactor was connected to gas chromatography (Chromatec-Crystal 5000.2), to analyze the gas phase formed after the process, using computer data processing and recording the signal of the detector for thermal conductivity. For saturation, gases were purged through a chromatographic column for 15 min. Gas separation was carried out on a 100 m long capillary column, at the following temperature conditions: 90 °C for 4 min, and then heating 10 °C/min to 250 °C. The temperature of the evaporator was 250 °C. The carrier gas was helium, with a flow rate of 15 mL/min.

The transformed experimental products were separated from water phase and prepared for further investigations by physical and chemical instrumental analysis methods, such as gas chromatography, SARA analysis, Rock-Eval, GC–MS, FTIR, and isotope mass spectroscopy (Figure 1).
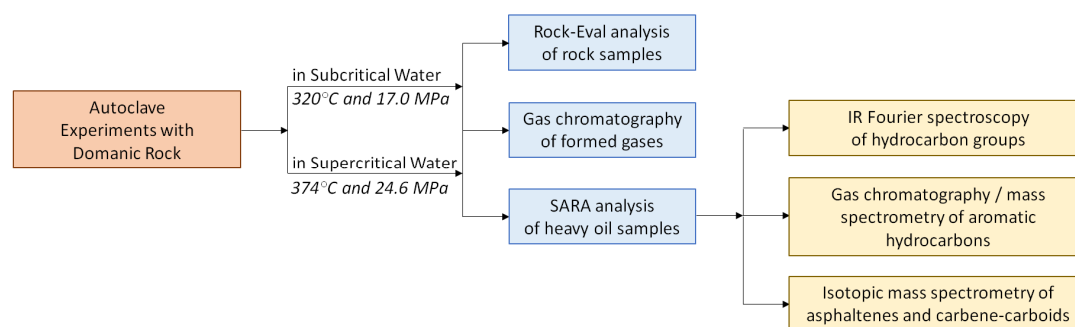


**Figure 1.** Experimental procedures scheme.

The total organic content in rock before and after the autoclave experiments was determined on elemental CHN-analyzer after dissolving carbonates from the given samples in hydrochloric acid. The transformation degree of organic matter in rock samples was evaluated via pyrolytic Rock-Eval analysis in a Pyro-GC–MS system (Frontier Lab EGA/PY-3030D, Agilent 7890B, Agilent 5977B), at the temperature range from 20 to 600 °C. The amount of thermally freed hydrocarbons in the sample in milligrams of hydrocarbons per gram of rock by temperature of 300 °C is designated as $S_1$. Residual oil potential, i.e., the content of hydrocarbons pyrolyzed from kerogen, was estimated by peak $S_2$. The maximum hydrocarbon yield within peak $S_2$ was determined by the temperature $T_{max}$. Based on these parameters, the oil generation potential of rock samples was evaluated, $GP = S_1 + S_2$, their productivity index, $PI = S_1/(S_1 + S_2)$, and the degree of kerogen conversion.

Extraction of heavy oil from the rock samples was done in Soxhlet for 72 h, with the mixture of organic solvents that was composed of chloroform, toluene, and isopropanol mixed in equal proportions. The rock extracts were separated according to SARA analysis into four fractions: saturated, aromatics, resins, and asphaltenes. Asphaltenes from the extracts were precipitated by aliphatic solvent n-hexane with the mass ratio of 1:40. The malthenes part of extracts was further separated in a liquid-chromatography column filled with previously calcined (at 425 °C) aluminum oxide. The saturated hydrocarbons, aromatics, and resins were eluted by hexane, toluene, and a mixture of benzene and isopropyl alcohol in equal proportions, respectively.

Aromatic hydrocarbons extracted from the heavy oil before and after autoclave experiments were studied by using a chromatomass-spectrometric system, including gas chromatography (Chromatec-Crystal 5000) with mass-selective detector ISQ with mass-selective detector ISQ LT manufactured by Thermo Fisher Scientific and software application Xcalibur for processing results. The chromatography was equipped with a capillary column, which was 30 m in length and 0.25 mm in diameter. The rate of gas-carrier (helium) phase and the temperature of injector was 1 mL/min and 310 °C, respectively. Moreover, the temperature was adjustable from 100 up to 300 °C, with a speed of 3 °C/min, and the process is isothermal through whole analysis. The potential of ion source—70 W and temperature 250 °C. Compounds were identified by digital library of NIST mass-spectrum and the literature data.

The structural group composition of SARA analysis fractions, saturated, aromatics, resins, asphaltenes, and carbonaceous substances, was determined by FTIR spectroscopy with Bruker Vector 22 IR spectrometer, in the range of 4000–400 $cm^{-1}$, with a resolution of 4 $cm^{-1}$. To assess changes in the structural-group composition of the products of the experiments, several parameters were used, defined as the ratio of the absorption values at the maximum of the corresponding absorption bands.

Investigation of the trace elements composition of rock samples, asphaltenes, and carbene–carboids was carried out in isotope mass spectrometer with inductively coupled plasma iCAP Qc manufactured by Thermo Fisher Scientific, Germany. The test sample weighed 100 mg. Concentrated hydrochloric, hydrofluoric, and nitric acid were added to the sample in Teflon autoclaves by dispensers. To account for the background, a mixture of acids without a sample was prepared. Hermetically sealed Teflon autoclaves were placed in the furnace of microwave digestion system, Mars 6 (CRM Corporation, USA), where samples were heated up to 210 °C for 30 min. After this, a boric acid solution was added to form complexes and transfer rare-earth fluorides to the solution. Teflon autoclaves were heated to 170 °C and kept at this temperature for 30 min. After cooling, the resulting solution was transferred to a test tube and diluted with deionized water and hydrochloric acid. The resulting solution was analyzed on a mass spectrometer pre-calibrated by using multi-element standards with a concentration in the range from 1 to 100 ppm of each element. The obtained concentration values were recalculated to the initial concentration, taking into account an empty sample, a sample, and dilution of the solution.

## 3. Results and Discussion

The results of pyrolytic Rock-Eval analysis and elemental analysis of oil-saturated rock samples before and after experiments in sub-CW and SCW conditions, as well as rock samples after extraction of heavy oil by organic solvents, are presented in Table 1.

By elemental analysis, the total organic content, $C_{org}$, in the source rock is 7.07%. According to Tisso and Welte [8], a rock sample with total organic content less than 3% corresponds to a class of good source rock. The initial rock sample is characterized by high oil-generation potential (22.17 mg HC/g of rock) and hydrogen index value (313.58 mg HC/g $C_{org}$). The value of $T_{max}$ (429 °C) indicates a low thermal maturity of OM. The value of the realized generation potential $S_1$, which is the fraction of free hydrocarbons in the rock, is rather low, at 1.75 mg/g of rock, which characterizes the low productivity index of this rock. It is proposed that the given sample is an excellent rock sample which did not pass through a high catagenesis stage.

**Table 1.** The results of pyrolytic Rock-Eval analysis of rock samples before and after autoclave experiments.

| Object | Parameters | | | | | | | |
|---|---|---|---|---|---|---|---|---|
| | $C_{org}$ | $H/C_{org}$ | $T_{max}$ | $S_1$ | $S_2$ | GP | PI | HI |
| Initial | 7.07 | 2.87 | 429 | 1.52 | 22.17 | 23.69 | 0.06 | 313.58 |
| * | 4.06 | 2.85 | 432 | 0.27 | 17.84 | 18.11 | 0.01 | 439.41 |
| Sub-CW | 6.98 | 2.18 | 432 | 1.06 | 17.79 | 18.85 | 0.06 | 254.87 |
| * | 4.02 | 1.28 | 434 | 0,27 | 17.01 | 17.28 | 0.02 | 302.13 |
| SCW | 4.08 | 5.44 | 435 | 1.79 | 1.95 | 3.74 | 0.48 | 47.79 |
| * | 3.12 | 5.50 | 433 | 0.39 | 2.42 | 2.82 | 0.14 | 77.56 |

* = the same sample after heavy oil extraction. $C_{org}$ = the total organic content in rock, wt%. $H/C_{org}$ = ratio of hydrogen to atomic organic carbon. $S_1$ = number of free hydrocarbons in the rock, mg HC/g of rock. $S_2$ = the number of hydrocarbons produced during the destruction of kerogen, mg HC/g of rock. $T_{max}$ = temperature at which the highest hydrocarbons yield intensity is observed within the peak $S_2$. GP = $S_1$ + $S_2$, the oil-generation potential, mg HC/g of rock. PI = $S_1/(S_1 + S_2)$, the productivity index, mg HC/g of rock. HI = $S_2/C_{opr}$ 100%, the hydrogen index, mg HC/g $C_{org}$. Sub-CW = subcritical water. SCW = supercritical water.

The sub-CW and SCW treatment of rock samples resulted in the transformation of organic matter, which was similar to natural maturation [34]. Residual oil potential, i.e., the content of hydrocarbons pyrolyzed from kerogen, decreases from 22.17 to 17.17 mg HC/g of rock in sub-CW, and to 1.95 mg HC/g of rock in SCW. This was also justified by the increase in $T_{max}$ value from 429 to 435 °C, and decrease in hydrogen index value from 313.58 to 47.79 mg HC/g $C_{org}$, which leads to an increase in the productivity index from 0.06 to 0.48 mg HC/g of rock in the SCW medium.

The decomposition of OM in SCW influenced the decrease in $C_{org}$, as well, from 7.07 to 4.08%. The atomic ratio of $H/C_{org}$ in the products of SCW treatment is higher than in initial rock sample. This indicates a participation of water in the conversion reactions of heavy components of OM into light alkane hydrocarbons. Similar results were obtained by Han et al. from an experimental investigation of high-temperature coal tar upgraded by SCW [35].

According to the SARA analysis presented in Table 2, a common behavior in group composition of extracts was revealed as the temperature of experiments was increased: The content of saturated fractions increased, while the content of resins decreased. In contrast to the initial extract, the content of aromatic hydrocarbons and asphaltenes after the treatment at sub-CW condition was increased, while the atomic $H/C_{org}$ ratio decreased. In the previous studies [31,32], an influence of sub-CW on improving extraction of asphaltenes and high-molecular n-alkanes $C_{22}$-$C_{30}$ from rock samples was shown. However, SCW effects decomposition of resins and asphaltenes with formation of low-molecular saturated hydrocarbons (33.91%wt.), as well as insoluble solid coal-like compounds, such as carbene–carboids (14.49%wt.). Formation of last may be the destruction result of alkyl chains of asphaltenes, as well as kerogen decomposition [36–38].

**Table 2.** The main characteristics of Domanic rock samples before and after the sub-CW and SCW experiments.

| Parameters | Object | | |
|---|---|---|---|
| | Initial | Sub-CW | SCW |
| Temperature of experiment, °C | - | 320 | 374 |
| Pressure of experiment, MPa | - | 17.0 | 24.6 |
| Gas yield, %wt. | - | 2.26 | 2.65 |
| Heavy oil yield, %wt. | 3.12 | 3.98 | 3.03 |
| Saturated, %wt. | 14.81 | 16.89 | 33.91 |
| Aromatics, %wt. | 19.17 | 22.74 | 14.33 |
| Resins, %wt. | 37.00 | 27.46 | 13.49 |
| Asphaltenes, %wt. | 29.02 | 32.91 | 23.78 |
| Carbene–carboids, %wt. | - | - | 14.49 |

Gas chromatography data for hydrocarbons and inorganic gases, formed during the process of OM transformation, are presented in Table 3. Uncondensed gases, formed from the shale rock in sub-CW and SCW conditions, are mainly composed of non-hydrocarbon gases such as $H_2$, $O_2$, and $CO_2$, as well as low-molecular hydrocarbon gases $C_1$-$C_4$ and alkenes $C_2$-$C_4$. The higher the temperature of the experiment, the more hydrocarbon gases, such as $CH_4$, $C_2H_6$, $C_3H_8$, $C_4H_8$, and n-$C_4H_{10}$, were released. It indicates that destructive processes via radical chain mechanism were carried out [30]. In experiments in the sub-CW medium, neither $C_2H_6$ nor $C_2H_4$ appear in the gas composition, which is consistent with the results obtained with extraction of Tumuji Oil Sand with sub-CW [23].

**Table 3.** The composition of formed gases after sub-CW and SCW experiments.

| Object | Gases Composition *, % vol. | | | | | | | | | |
|---|---|---|---|---|---|---|---|---|---|---|
| | $H_2$ | $O_2$ | $CO_2$ | $CH_4$ | $C_2H_4$ | $C_2H_6$ | $C_3H_6$ | $C_3H_8$ | $C_4H_8$ | n-$C_4H_{10}$ |
| Sub-CW | 0.23 | 10.89 | 83.76 | 3.96 | 0.00 | 0.00 | 0.12 | 0.02 | 0.08 | 0.25 |
| SCW | 0.51 | 9.98 | 64.60 | 11.66 | 0.12 | 5.96 | 0.00 | 3.93 | 0.36 | 0.99 |

* Excluding nitrogen.

The high content of $CO_2$ in the composition of the released gases may be due to decomposition of OM and carbonate rock minerals in sub-CW and SCW. In Reference [39], the conduction of oxidation-reduction reactions of OM and mineral components of shale rocks in the presence of water with production of CO and $CO_2$ gases was reported. The presence of $O_2$ in the composition of formed gases also justifies the conduction of oxidation-reduction reactions.

The GC–MS method was applied to gain information about individual composition of aromatic fractions (Figure 2). The concentration of methyl- and ethyl-substituted benzothiophenes (peaks 11 and 15) prevailed in the initial extracts. The concentration of 7-ethylbenzothhiophene/5-ethylbenzothiophene (peak 11) significantly decreased at a temperature of 320 °C. However, the relative concentration of 2,5,7-trimethyl-benzo[b]thiophene and 7-ethyl-2-methylbenzo[b]thiophene (peaks 15 and 14) increased, and a peak of 2,5-dimethylbenzothiophene appeared (peak 8). The important changes were observed in the composition of aromatic hydrocarbons after the treatment of rock at SCW condition (374 °C and 24.6 MPa).
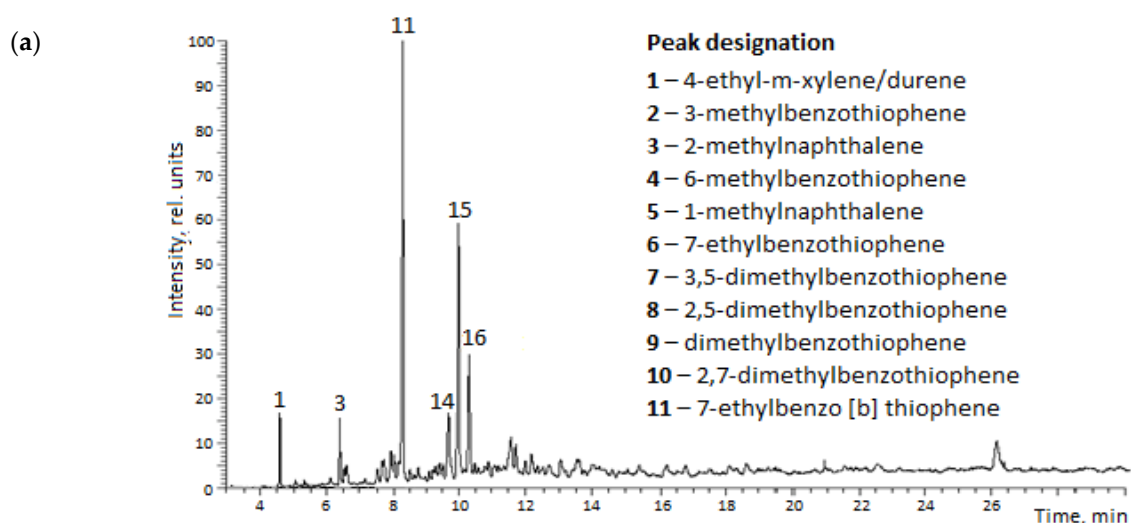


**(a)**

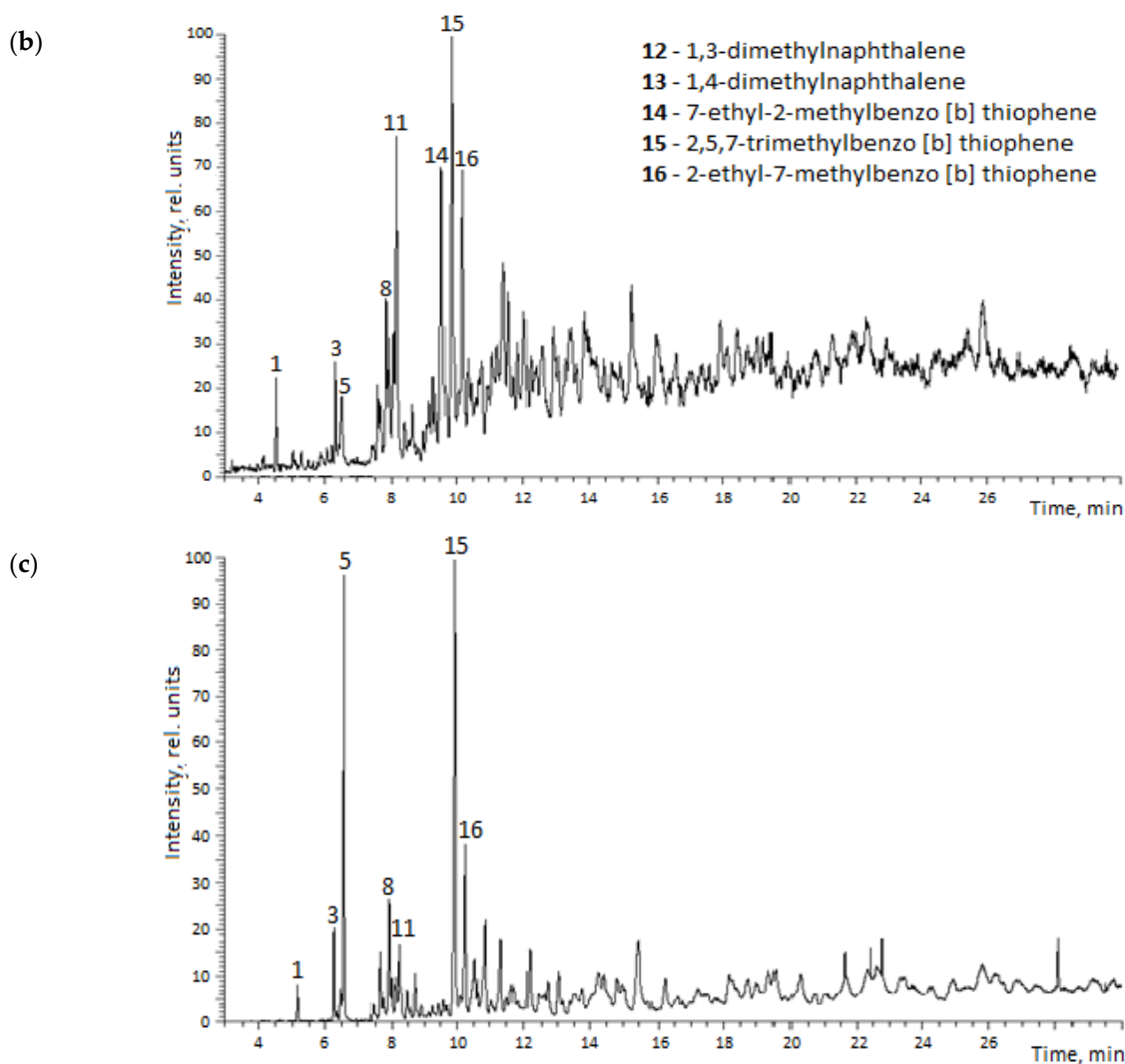Peak designation

1 – 4-ethyl-m-xylene/durene
2 – 3-methylbenzothiophene
3 – 2-methylnaphthalene
4 – 6-methylbenzothiophene
5 – 1-methylnaphthalene
6 – 7-ethylbenzothiophene
7 – 3,5-dimethylbenzothiophene
8 – 2,5-dimethylbenzothiophene
9 – dimethylbenzothiophene
10 – 2,7-dimethylbenzothiophene
11 – 7-ethylbenzo [b] thiophene

**Figure 2.** *Cont.*

**Figure 2.** Total ion current (TIC) chromatogram of aromatic hydrocarbons: (**a**) initial, (**b**) sub-CW, and (**c**) SCW.

The specific features of molecular-mass distributions of aromatic compounds in experimental products were illustrated in diagram (Figure 3). There were no 7-ethylbenzothhiophene/5-ethyl-benzo-thiophene and 7-ethyl-2-methylbenzo[b]thiophene (peaks 11 and 14) observed in experimental products. However, an intensive peak corresponding to 1-methyl-naphtalene (peak 5) was identified. This confirms the conduction of destructive processes with detachment of alkyl substitutes and probably destruction of aromatic heterocyclic compounds.
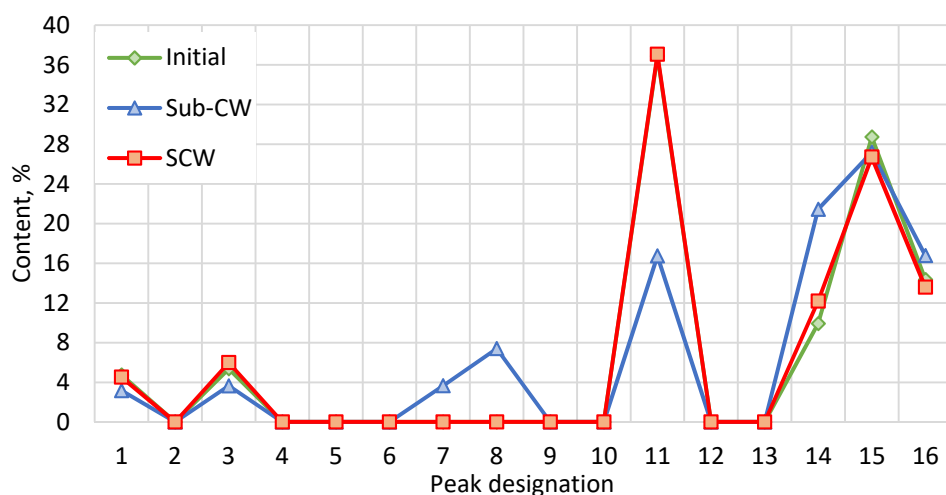
**Figure 3.** Molecular-mass distribution of aromatic compounds before and after sub-CW and SCW treatments, determined by total ion current (TIC).

Figure 4 shows the mass chromatograms of aromatic compounds with characteristic ions at *m/z* 184 + 198 + 212 (dibenzothiophenes) within the range of 10–25 min. Mass chromatograms confirm the data obtained by the total ion current (TIC) about destruction of more high-molecular aromatic compounds such as methyldibenzothiophenes $C_{13}H_{10}S$ and alkylated $C_2$-dibenzothiophenes $C_{14}H_{12}S$ in sub-CW and SCW. This fact indicates that part of the associated structure of heavy aromatic components was depolymerized and transformed into the light aromatic compounds at sub-CW and SCW conditions, as a result of the detachment of alkyl substituents and the destruction of aromatic fragments.
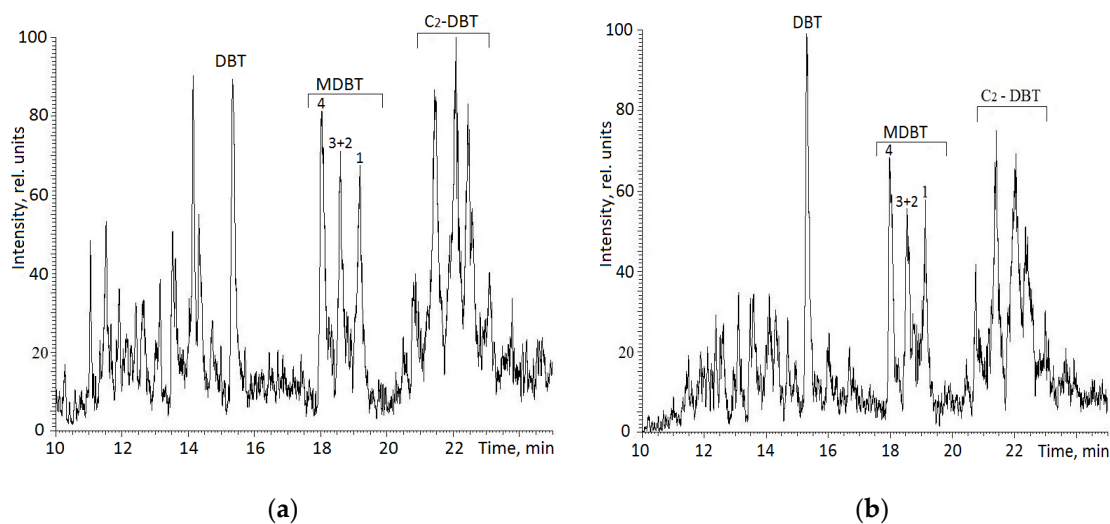


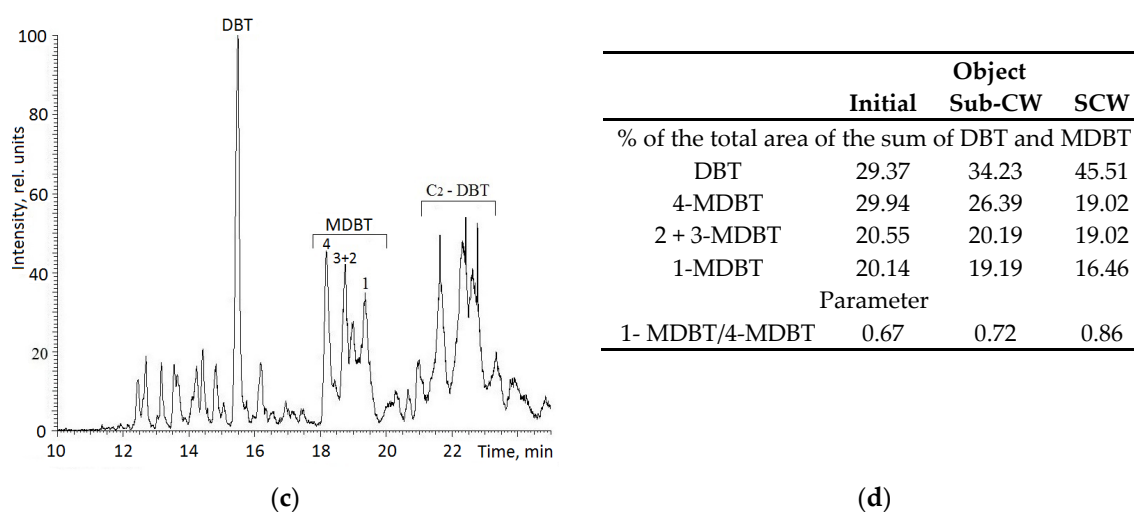(**a**)　　　　　　　　　　　　　　　　　　(**b**)

**Figure 4.** *Cont.*

(c)

| | Object | | |
|---|---|---|---|
| | **Initial** | **Sub-CW** | **SCW** |
| % of the total area of the sum of DBT and MDBT | | | |
| DBT | 29.37 | 34.23 | 45.51 |
| 4-MDBT | 29.94 | 26.39 | 19.02 |
| 2 + 3-MDBT | 20.55 | 20.19 | 19.02 |
| 1-MDBT | 20.14 | 19.19 | 16.46 |
| Parameter | | | |
| 1- MDBT/4-MDBT | 0.67 | 0.72 | 0.86 |

(d)

**Figure 4.** Mass chromatograms of aromatic hydrocarbons, (**a**) initial, (**b**) sub-CW, and (**c**) SCW at *m/z* 184 + 198 + 212 (dibenzothiophenes), and (**d**) components peak area and parameters. The numbers refer to the number of carbon atoms in alkyltrimethylbenzene molecules. DBT, MDBT, and $C_2$-DBT are the elution regions of dibenzothiophene, methyldibenzothiophene isomers, and $C_2$-dibenzothiophenes, respectively.

Heteroatomic compounds 1- and 4-methyl-dibenzothiphene are stable enough for degradation processes [40]. Bennete et al. imply that 4-methyl-dibenzothiophene (4-MDBT) is less stable for degradation than 1-methyl-dibenzothiophene (1-MDBT) [41]. That is the reason why the parameter 1-MDBT/4-MDBT (Figure 4d) is an indirect indicator for decomposition degree of kerogen and further destruction of its high-molecular fragments. For transformed samples, the given ratio increased from 0.67 to 0.86, in contrast to the initial rock sample (Figure 4c).

The studies about the SCW technique for shale rock require the selection of a method that can provide knowledge about the converted products' structure and composition. One of the informative instrumental methods is considered the FTIR spectroscopy, which allows for the evaluation of transformations not only in various hydrocarbons, but also in functional groups, at natural and technology-related processes [42,43]. The IR spectra of the obtained hydrocarbon groups are presented in Figure 5. Table 4 shows the FTIR structural parameters of hydrocarbon groups as a function of the experimental conditions.
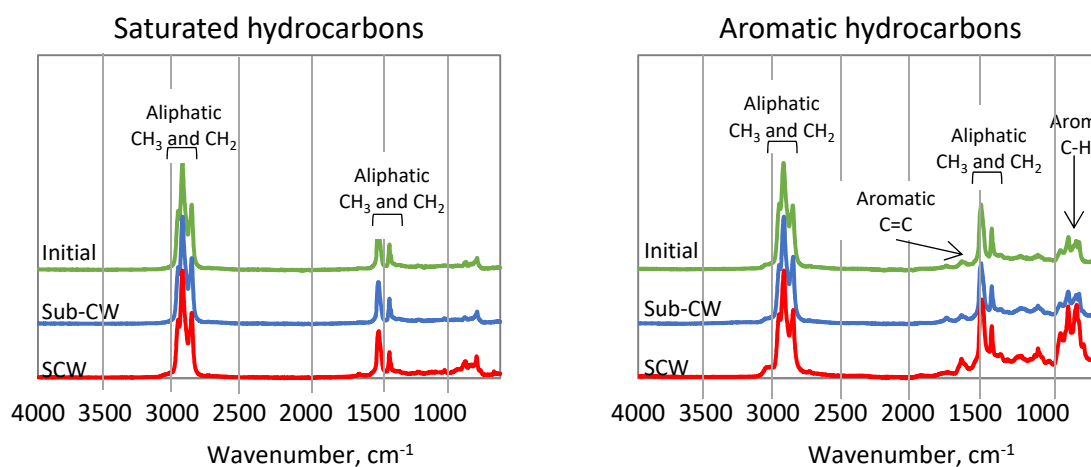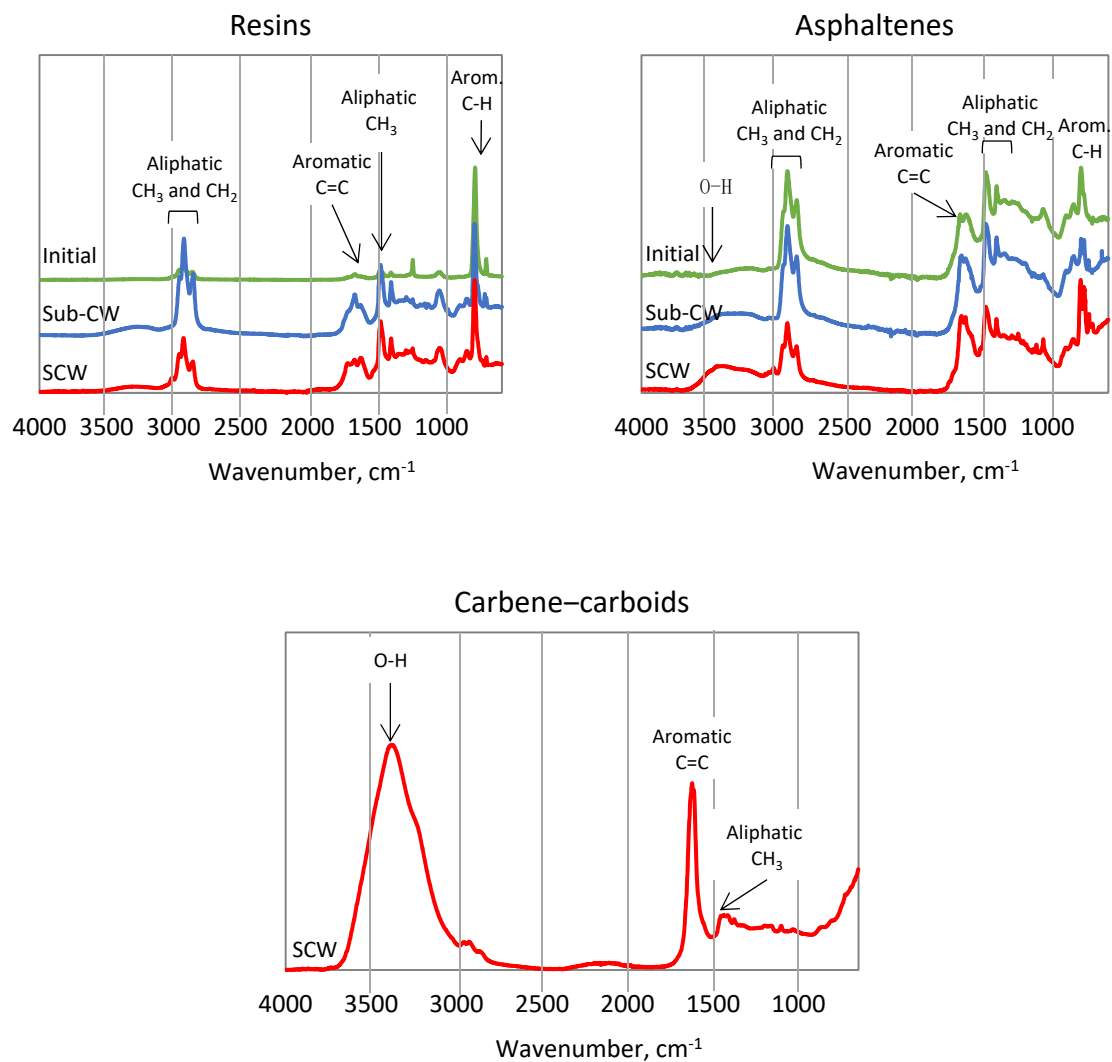


**Figure 5.** *Cont.*

**Figure 5.** IR spectra of saturated and aromatic hydrocarbons, resins, asphaltenes, and carbene–carboids of Domanic rock before and after sub-CW and SCW experiments.

The composition of saturated hydrocarbons, according to IR spectroscopy, includes aliphatic $CH_2$ and $CH_3$ structural groups at 1380–1465 cm$^{-1}$. With an increase in the experimental temperature, the values of the spectral indices of the fractions of saturated hydrocarbons practically do not change.

*A-Factor* is an indicator determining the ratio of intensities of IR absorbance bands aliphatic $CH_2$ and $CH_3$ structures to aromatic C=C bonds [44–46].

$$A - Factor = \frac{I\left(2857cm^{-1}\right) + I\left(2925cm^{-1}\right)}{I(2857cm^{-1}) + I(2925cm^{-1}) + I(1630cm^{-1})}$$

*C-Factor* represents the intensity of the absorbance band of oxygenated functional groups versus aromatic ring in hydrocarbons [44].

$$C - Factor = \frac{I\left(1710 \ cm^{-1}\right)}{I(1710 \ cm^{-1}) + I(1630 \ cm^{-1})}$$

**Table 4.** Structural parameters of hydrocarbon groups before and after sub-CW and SCW experiments.

| Object | Structural Parameters | | | | |
|---|---|---|---|---|---|
| | CH$_3$/CH$_2$ Ratio | A-Factor | C-Factor | Aromaticity | Degree of Condensation |
| Saturated hydrocarbons | | | | | |
| Initial | 0.04 | 0.55 | 0.99 | 0.34 | 1.17 |
| Sub-CW | 0.04 | 0.53 | 0.99 | 0.37 | 1.14 |
| SCW | 0.04 | 0.54 | 0.97 | 0.24 | 1.45 |
| Aromatic hydrocarbons | | | | | |
| Initial | 0.62 | 0.95 | 0.34 | 1.19 | 0.88 |
| Sub-CW | 0.57 | 0.95 | 0.42 | 1.21 | 0.83 |
| SCW | 0.63 | 0.89 | 0.23 | 1.15 | 0.55 |
| Resins | | | | | |
| Initial | 0.70 | 0.86 | 0.39 | 3.28 | 0.94 |
| Sub-CW | 0.61 | 0.84 | 0.42 | 1.09 | 0.38 |
| SCW | 0.71 | 0.71 | 0.44 | 2.89 | 0.40 |
| Asphaltenes | | | | | |
| Initial | 0.60 | 0.74 | 0.21 | 0.46 | 0.19 |
| Sub-CW | 0.62 | 0.71 | 0.17 | 0.65 | 0.24 |
| SCW | 0.67 | 0.62 | 0.16 | 1.26 | 0.27 |
| Carbene–carboids | | | | | |
| SCW | 0.99 | 0.28 | 0.09 | 3.16 | 0.22 |

*CH$_3$/CH$_2$ ratio* is an indicator of the length of the aliphatic chain and the branching degree of aliphatic fragments [47,48].

$$CH_3/CH_2\ ratio = \frac{I\left(2957\ cm^{-1}\right)}{I\left(2925\ cm^{-1}\right)}$$

*Aromaticity* is related to the relative peak intensity of aromatic C–H stretching versus aliphatic C–H stretching [49].

$$Aromaticity = \frac{I\left(3050\ cm^{-1}\right)}{I\left(2897\ cm^{-1}\right)}$$

The degree of condensation reflects the degree of aromatic substitution as compared to ring condensation [50,51]. The degree of condensation is determined as the intensity of aromatic C–H stretching divided to aromatic C=C stretching intensity. With an increase in the degree of ring condensation, the value of this parameter decreases.

$$Degree\ of\ condensation\ (DOC) = \frac{I\left(3050\ cm^{-1}\right)}{I\left(1600\ cm^{-1}\right)}$$

The composition of saturated hydrocarbons, according to IR spectroscopy, includes aliphatic CH$_2$ and CH$_3$ structural groups at 1380–1465 cm$^{-1}$. With an increase in the experimental temperature, the values of the spectral indices of the fractions of saturated hydrocarbons practically do not change.

In the spectra of aromatic hydrocarbons, absorption bands of 1600 cm$^{-1}$ и650–900 cm$^{-1}$ are identified corresponding to C=C and C–H bonds in aromatic structures. The intense band in the region of 1380 cm$^{-1}$ characterizes the CH$_3$ structures stretching vibrations in aromatic hydrocarbons. Low-intensity bands also appear with peaks at 1710 and 1030 cm$^{-1}$, which are characteristic of stretching vibrations of the C–O bonds in the carbonyl groups and S=O bonds in the sulfoxide groups. With increasing temperature, the aromatic triplet in the range of 650–900 cm$^{-1}$ in the IR spectra of aromatic hydrocarbons becomes more intense. Aromatic hydrocarbons after the experiment in SCW condition are characterized by a low value of DOC (0.55 versus 0.88). This indicates that C=C bonds of aromatic rings prevail over C-H bonds in aromatic structures. In the resins' spectra before

and after the experiments, an absorption band of 870–880 cm$^{-1}$ is detected, which indicates the presence of 1, 3-substituted aromatic rings. The band of 810–820 cm$^{-1}$ reflects the presence of 1,2,3,4 or 1,4-substituted benzene fragments in the composition of the resins, while the band of 750 cm$^{-1}$ represents monosubstituted structures. After autoclave experiments, resins become more aromatic, as evidenced by an increase in the intensity of the 750 and 1600 cm$^{-1}$ absorption bands. Decreasing the values of DOC from 0.94 to 0.4 is due to aromatization process in SCW. The transformed resins are distinguished not only by an increase in the content of aromatics, but also aliphatic by CH$_3$ and CH$_2$ structures, corresponding to 2857–2957 and 1380–1465 cm$^{-1}$ absorption bands. Oxidation of resins in SCW increases the value of C-factor from 0.39 to 0.44 that characterizes a ratio of oxygenated functional groups to aromatic hydrocarbons.

The hexane insoluble asphaltenes fraction in the initial rock was 29.02 wt.%. According to IR spectroscopy (Figure 3), asphaltenes include polycondensed aromatic fragments containing carbonyl, carboxyl, and aliphatic functional groups. The spectrum of asphaltenes after sub-CW and SCW experiments differs from the spectrum of the initial asphaltenes by decreasing intensity of 2857–2957 cm$^{-1}$ bands, corresponding to aliphatic CH$_3$ and CH$_2$ structures. Increasing aromaticity and decreasing A-Factor values indicate the conduction of aromatization processes of asphaltenes in SCW.

Oxygen-containing C-O bonds in the asphaltenes' structure after SCW experiment are destroyed, which is indicated by a decrease in the intensity of the absorption bands of C–O–C and S=O functional groups at 1160 and 1030 cm$^{-1}$. It is also confirmed by decreasing the C-factor from 0.21 to 0.16. However, the content of O–H structures in transformed asphaltenes increase (from the intensity 3342 cm$^{-1}$ absorption band). A significant number of such oxygen-containing O–H structures was observed in carbene–carboids, the formation of which may be due to the following reasons. Firstly, kerogen of Domanic shales contains a significant amount of oxygen. Particularly, oxygen-containing bonds are revealed to be dominating in Domanic shales of Middle Volga [52]. Kerogen contains monosaccharide units of n-alkyl chains, substituted by alcohol, ketone, and aldehyde groups [52], as well as long-chain C$_{19}$–C$_{32}$ carboxylic acids [53]. Hence, during decomposition of kerogen structure free oxygen and oxygen-containing fragments, which were in fractions of asphaltenes and carbene–carboids, may be released. Secondly, water may participate in oxidation-reduction reactions of transforming heavy hydrocarbons in the rock composition [39]. Thus, carbene–carboids were formed in SCW due to kerogen oxidative destruction. The specific feature of such compounds is the absence of long alkyl chains and the presence of only short CH$_3$ structures, which is confirmed by a high value of CH$_3$/CH$_2$ Ratio—0.99.

In connection with the development of Domanic strata and their high enrichment with trace elements [54,55], it is of interest to study their distribution both in the composition of the recovered oil and in the rocks. Metals create many problems in the extraction and processing of heavy hydrocarbons, for example, in terms of their impact on the environment and processing processes, poisoning the catalysts. At the same time, their positive influence can be distinguished—in particular, the possibility of associated extraction from Domanic rocks of a number of valuable industrial and rare metals, such as V, Ni, Co, Mo, etc., and in addition, the catalytic properties of metals in rocks under exposure on the layer of thermal methods in the processes of its development. Information on the distribution of trace elements in rocks allows us to draw conclusions about the genesis of hydrocarbons and about processes that affect the formation of their composition [56].

The following trace elements were determined by isotope mass spectrometry in the rocks, asphaltenes, and carbene–carboids: Ti, V, Cr, Mn, Fe, Co, Ni, Cu, Zn, Li, Cd, Sb, Ba, Mo, Ga, Ge, As, and Se (Figure 6). The predominant trace elements in the composition of the rocks are Ti, Fe, Ni, and Zn. Asphaltenes contain the highest concentration of V, Fe, Ni, and Zn. The impact of SCW on Domanic rock leads to a decrease in the concentration of V in the structure of asphaltenes from 1442 to 634 ppm and Ni from 852 to 508 ppm, compared with asphaltenes from the original rock sample. This is consistent with previously obtained electron paramagnetic resonance data [32], which showed a decrease in the VO$^{2+}$ concentration in the converted asphaltenes after processing the rock

in the SCW medium. It should be noted that, in the composition of formed carbene–carboids, the Ni content significantly prevails over the V content in contrast to asphaltenes. In the composition of carbene–carboids and transformed asphaltenes, as well as in rock samples, the highest concentrations occur in trace elements V, Mn, Fe, Ni, and Zn, which are probably associated with the transition of trace elements from kerogen and rock minerals to the composition of asphaltenes and carbene–carboids in the sub-CW and SCW environment. Thus, trace elements in rocks and experiment products can exhibit catalytic activity in transformation of high-molecular components of heavy oil and insoluble kerogen in sub-CW and SCW.



**Figure 6.** Distribution of trace elements in (**a**) rock samples, (**b**) asphaltenes, and (**c**) carbene–carboids of Domanic shales before and after sub-CW and SCW experiments.

## 4. Conclusion

Our work has led us to conclude that sub-CW and SCW provide conduction of intensive processes on transformation of high-molecular components of heavy oil and insoluble kerogen of Domanic shales into light mobile crude oil. The thermal processes of kerogen decomposition and tar-asphaltene substances' destruction occur more intensively in the SCW than in the sub-CW medium, and they lead to a decrease in the oil-generation potential of rock from 23.7 to 3.7 mg/g and an increase

in the productivity index from 0.06 to 0.48 mg/g. In the products of the experiment in SCW, an increase in saturated hydrocarbons content was found to increase by more than two times. In sub-CW condition at 320 °C and 17 MPa, OM is particularly decomposed, and some parts of asphaltenes and high-molecular n-alkanes $C_{22}$-$C_{30}$ are extracted. The products of the experiments differ in the content and composition of aromatic hydrocarbons from the initial ones with an increased content of light hydrocarbons of 2,5-dimethylbenzothiophene $C_{10}H_{10}S$ and 1-methylnaphthalene $C_{11}H_{10}$ and a reduced content of higher-molecular-weight aromatic compounds, such as 7-ethyl-2-methylbenzo[b]thiophene $C_{11}H_{12}S$, methyldibenzothiophenes $C_{13}H_{10}S$, and alkylated $C_2$-dibenzothiophenes $C_{14}H_{12}S$. Intensive decomposition of heavy aromatics, resins, and asphaltenes, as well as insoluble kerogen in SCW, is followed by the formation of insoluble coal-like compounds such as carbene–carboids. Their formation is due to kerogen oxidative destruction, which is confirmed by increasing intensity of absorption band in FTIR spectra, corresponding to O–H structures of asphaltenes and carbene–carboids after experiments. The distribution of trace elements in rocks, asphaltenes, and carbene–carbides was shown before and after sub-CW and SCW exposure. It was established that SCW affects the decomposition of asphaltenes' structures containing V and Ni trace elements. In the composition of transformed asphaltenes and formed carbene–carboids, as well as in rock samples, the highest concentrations occur in trace elements V, Mn, Fe, Ni, and Zn, which are probably associated with the transition of trace elements from kerogen and rock minerals to the composition of asphaltenes and carbene–carboids in the sub-CW and SCW environment.

The results of this study allow us to expand our knowledge of the transformation of heavy oil components and kerogen in sub-CW and SCW environment to select the optimal conditions for the development of these low-permeability organic-rich Domanic deposits.

**Author Contributions:** Description of the results, Z.R.N. and G.P.K.; data curation, A.V.V.; experimental analysis, R.D. and A.E.C. All authors have read and agreed to the published version of the manuscript.

**Conflicts of Interest:** The authors declare no conflict of interest.

## References

1. Zou, C.; Zhai, G.; Zhang, G.; Wang, H.; Zhang, G.; Li, J.; Wang, Z.; Wen, Z.; Ma, F.; Liang, Y.; et al. Formation, distribution, potential and prediction of global conventional and unconventional hydrocarbon resources. *Pet. Explor. Dev.* **2015**, *42*, 14–28. [CrossRef]

2. Chengzao, J.; Zheng, M.; Zhang, Y. Unconventional hydrocarbon resources in China and the prospect of exploration and development. *Pet. Explor. Dev.* **2012**, *39*, 139–146.

3. Zou, C.N.; Zhu, R.K.; Wu, S.T.; Yang, Z.; Tao, S.Z.; Yuan, X.J.; Hou, L.H.; Yang, H.; Xu, C.C.; Li, D.H. Types, characteristics, genesis and prospects of conventional and unconventional hydrocarbon accumulations: Taking tight oil and tight gas in China as an instance. *Acta Pet. Sin.* **2012**, *33*, 173–187.

4. Khisamov, R.S.; Bazarevskaya, V.G.; Tarasova, T.I.; Mikhailova, O.V.; Mikhailov, S.N. Geochemical evidence for petroleum potential of Domanic deposits in the Republic of Tatarstan (Russian). *Oil Ind. J.* **2016**, *2016*, 10–13.

5. Khisamov, R.S.; Zakirov, I.S.; Zakharova, E.F.; Bazarevskaya, V.G.; Abusalimova, R.R.; Timirov, D.A. Experience of studying and development of domanic deposits on the example of bavlinskoye field of the republic of Tatarstan. *Neft. Khozyaystvo Oil Ind.* **2018**, *11*, 78–83. [CrossRef]

6. Kayukova, G.P.; Mikhaylova, A.N.; Kosachev, I.P.; Morozov, V.P.; Vakhin, A.V. Gidrotermal'nyye prevrashcheniya organicheskogo veshchestva vysokouglerodistoy domanikovoy porody pri raznykh temperaturakh v uglekislotnoy srede. *Neftekhimiya* **2020**, *60*, 307–320.

7. Bushnev, D.A.; Burdel'naya, N.S.; Shanina, S.N.; Makarova, E.S. Generation of hydrocarbons and hetero compounds by sulfur-rich oil shale in hydrous pyrolysis. *Pet. Chem.* **2004**, *44*, 416–425.

8. Tissot, B.P.; Welte, D.H. *Petroleum Formation and Occurrence*, 2nd ed.; Springer: Berlin Heidelberg, Germany, 1984; p. 702. [CrossRef]

9. Khisamov, R.S.; Bazarevskaya, V.G.; Yartiev, A.F.; Tarasova, T.I.; Gibadullina, O.G.; Mikhailova, O.V. Oil potential of Domanic productive formations in territory of Leninogorskneft activities. *Neft. Khozyaystvo Oil Ind.* **2015**, *7*, 10–14.

10. Stoupakova, A.V.; Kalmykov, G.A.; Korobova, N.I.; Fadeeva, N.P.; Gatovskii, Y.A.; Suslova, A.A.; Sautkin, R.S.; Pronina, N.V.; Bolshakova, M.A.; Zavyalova, A.P.; et al. Domanic deposits of the Volga-Ural basin—Types of section, formation conditions and prospects of oil and gas potential. *Georesursy* **2017**, *19*, 112–124. [CrossRef]

11. Kayukova, G.P.; Mikhailova, A.M.; Feoktistov, D.A.; Morozov, V.P.; Vakhin, A.V. Conversion of the organic matter of domanic shale and permian bituminous rocks in hydrothermal catalytic processes. *Energy Fuels* **2017**, *31*, 7789–7799. [CrossRef]

12. Vakhin, A.V.; Onishchenko, Y.V.; Chemodanov, A.E.; Sitdikova, L.M.; Nurgaliev, D.K. Thermal transformation of bitumoid of Domanic formations of Tatarstan (Russian). *Oil Ind. J.* **2016**, *2016*, 32–34.

13. Galimov, E.M.; Kamaleeva, A.I. Source of hydrocarbons in the supergiant Romashkino oilfield (Tatarstan): Recharge from the crystalline basement or source sediments? *Geochemistry Int.* **2015**, *53*, 95–112. [CrossRef]

14. Whitehead, J.C.; Williams, D.F. Solvent extraction of coal by a supercritical gases. *J. Inst. Fuel* **1975**, *48*, 182.

15. Funazukuri, T.; Yokoi, S.; Wakao, N. Supercritical fluid extraction of Chinese Maoming oil shale with water and toluene. *Fuel* **1988**, *67*, 10–14. [CrossRef]

16. Yanik, J.; Yüksel, M.; Sağlam, M.; Olukçu, N.; Bartle, K.; Frere, B. Characterization of the oil fractions of shale oil obtained by pyrolysis and supercritical water extraction. *Fuel* **1995**, *74*, 46–50. [CrossRef]

17. Luik, L.; Luik, H.; Palu, V.; Kruusement, K.; Tamvelius, H. Conversion of the Estonian fossil and renewable feedstocks in the medium of supercritical water. *J. Anal. Appl. Pyrolysis* **2009**, *85*, 492–496. [CrossRef]

18. Kruse, A.; Dinjus, E. Hot compressed water as reaction medium and reactant: Properties and synthesis reactions. *J. Supercrit. Fluids* **2007**, *39*, 362–380. [CrossRef]

19. Siskin, M.; Katritzky, A.R. Review of the reactivity of organic compounds with oxygen-containing functionality in superheated water. *J. Anal. Appl. Pyrolysis* **2000**, *54*, 193–214. [CrossRef]

20. Akiya, N.; Savage, P.E. Roles of water for chemical reactions in high-temperature water. *Chem. Rev.* **2002**, *102*, 2725–2750. [CrossRef]

21. Al-alla, R.A.; Nassef, E. Extraction of Oil from Egyptian Oil Shale. *J. Pet. Environ. Biotechnol.* **2015**, *6*, 6–10. [CrossRef]

22. Abourriche, A.; Oumam, M.; Hannache, H.; Adil, A.; Pailler, R.; Naslain, R.; Birot, M.; Pillot, J.P. Effect of toluene proportion on the yield and composition of oils obtained by supercritical extraction of Moroccan oil shale. *J. Supercrit. Fluids* **2009**, *51*, 24–28. [CrossRef]

23. Meng, M.; Hu, H.; Zhang, Q.; Ding, M. Extraction of tumuji oil sand with sub- and supercritical water. *Energy Fuels* **2006**, *20*, 1157–1160. [CrossRef]

24. Arcelus-Arrillaga, P.; Pinilla, J.L.; Hellgardt, K.; Millan, M. Application of water in hydrothermal conditions for upgrading heavy oils: A review. *Energy Fuels* **2017**, *31*, 4571–4587. [CrossRef]

25. Canıaz, R.O.; Arca, S.; Yaşar, M.; Erkey, C. Refinery bitumen and domestic unconventional heavy oil upgrading in supercritical water. *J. Supercrit. Fluids* **2019**, *152*, 1–10. [CrossRef]

26. Daud, A.R.M.; Pinilla, J.L.; Arcelus-arrillaga, P.; Hellgardt, K.; Kandiyoti, R.; Millan, M. Heavy oil upgrading in subcritical and supercritical water: Studies on model compounds. *Am. Chem. Soc. Div. Energy Fuels* **2012**, *57*, 22.

27. Gudiyella, S.; Lai, L.; Borne, I.H.; Tompsett, G.A.; Timko, M.T.; Choi, K.H.; Alabsi, M.H.; Green, W.H. An experimental and modeling study of vacuum residue upgrading in supercritical water. *AIChE J.* **2018**, *64*, 1732–1743. [CrossRef]

28. Cheng, Z.-M.; Ding, Y.; Zhao, L.-Q.; Yuan, P.-Q.; Yuan, W.-K. Effects of supercritical water in vacuum residue upgrading. *Energy Fuels* **2009**, *23*, 3178–3183. [CrossRef]

29. Canel, M.; Missal, P. Extraction of solid fuels with sub-and supercritical water. *Fuel* **1994**, *73*, 1776–1780. [CrossRef]

30. Olukcu, N.; Yanik, J.; Saglam, M.; Yuksel, M.; Karaduman, M. Solvent effect on the extraction of Beypazari oil shale. *Energy Fuels* **1999**, *13*, 895–902. [CrossRef]

31. Nasyrova, Z.R.; Kayukova, G.P.; Onishchenko, Y.V.; Morozov, V.P.; Vakhin, A.V. Conversion of high-carbon Domanic Shale in sub-and supercritical water. *Energy Fuels* **2020**, *34*, 1329–1336. [CrossRef]

32.    Nasyrova, Z.R.; Kayukova, G.P.; Khasanova, N.M.; Vakhin, A.V. Transformation of organic matter of domanik rock from the Romashkino oilfield in sub- and supercritical water. *Pet. Chem.* **2020**, *60*. [CrossRef]

33.    Linstrom, P.J.; Mallard, W.G.; Stein, S.E. NIST Chemistry WebBook (NIST Standard Reference Database vol 69). 2017. Available online: https://webbook.nist.gov/chemistry/ (accessed on 1 March 2020).

34.    Lopatin, N.V.; Emets, T.P. *Pyrolysis in Oil and Gas Geochemistry (in Russian)*; Nauka: Moscow, Russia, 1987.

35.    Han, L.; Zhang, R.; Bi, J. Experimental investigation of high-temperature coal tar upgrading in supercritical water. *Fuel Process. Technol.* **2009**, *90*, 292–300. [CrossRef]

36.    Kayukova, G.P.; Kiyamova, A.M.; Mikhailova, A.N.; Kosachev, I.P.; Petrov, S.M.; Romanov, G.V.; Sitdikova, L.M.; Plotnikova, I.N.; Vakhin, A.V. Generation of hydrocarbons by hydrothermal transformation of organic matter of Domanik rocks. *Chem. Technol. Fuels Oils* **2016**, *52*, 149–161. [CrossRef]

37.    Antipenko, V.R.; Bakanova, O.S.; Kashapov, R.S. Kharakteristika termicheskoy ustoychivosti masel prirodnykh bitumov i neftey. *Izv. Tomsk. Politekh. Univ. Inzhiniring Georesursov.* **2019**, *330*, 152–160. [CrossRef]

38.    Kayukova, G.P.; Mikhailova, A.N.; Kosachev, I.P.; Eskin, A.A.; Morozov, V.I. Effect of the natural minerals pyrite and hematite on the transformation of Domanik rock organic matter in hydrothermal processes. *Pet. Chem.* **2019**, *59*, 24–33. [CrossRef]

39.    Fedyaeva, O.N.; Antipenko, V.R.; Dubov, D.Y.; Kruglyakova, T.V.; Vostrikov, A.A. Non-isothermal conversion of the Kashpir sulfur-rich oil shale in a supercritical water flow. *J. Supercrit. Fluids* **2016**, *109*, 157–165. [CrossRef]

40.    Peter, K.E.; Walter, C.C.; Moldowan, M. *The Biomarker Guide, Volume 2—Biomarkers and Isotopes in Petroleum Exploration and Earth History*; Cambridge University Press: Cambridge, UK, 2005.

41.    Bennett, B.; Adams, J.J.; Larter, S.R. Oil fingerprinting for production allocation: Exploiting the natural variations in fluid properties encountered in heavy oil and oil sand reservoirs. In Proceedings of the Frontiers + Innovation – 2009 CSPG CSEG CWLS Convention, Calgary, AB, Canada, 4–8 May 2009; pp. 157–160.

42.    Jameel, A.G.A.; Han, Y.; Brignoli, O.; Telalović, S.; Elbaz, A.M.; Im, H.G.; Roberts, W.L.; Sarathy, S.M. Heavy fuel oil pyrolysis and combustion: Kinetics and evolved gases investigated by TGA-FTIR. *J. Anal. Appl. Pyrolysis* **2017**, *127*, 183–195. [CrossRef]

43.    Zhao, R.; Zhang, C.; Yang, F.; Heng, M.; Shao, P.; Wang, Y. Influence of temperature field on rock and heavy components variation during in-situ combustion process. *Fuel* **2018**, *230*, 244–257. [CrossRef]

44.    Ganz, H.; Kalkreuth, W. Application of infrared spectroscopy to the classification of kerogentypes and the evaluation of source rock and oil shale potentials. *Fuel* **1987**, *66*, 708–711. [CrossRef]

45.    Craddock, P.R.; Le Doan, T.V.; Bake, K.; Polyakov, M.; Charsky, A.M.; Pomerantz, A.E. Evolution of kerogen and bitumen during thermal maturation via semi-open pyrolysis investigated by infrared spectroscopy. *Energy Fuels* **2015**, *29*, 2197–2210. [CrossRef]

46.    Iglesias, M.J.; Jimenez, A.; Laggoun-Défarge, F.; Suarez-Ruiz, I. FTIR study of pure vitrains and associated coals. *Energy Fuels* **1995**, *9*, 458–466. [CrossRef]

47.    Lin, R.; Ritz, G.P. Studying individual macerals using ir microspectrometry, and implications on oil versus gas/condensate proneness and "low-rank" generation. *Org. Geochem.* **1993**, *20*, 695–706. [CrossRef]

48.    Lis, G.P.; Mastalerz, M.; Schimmelmann, A.; Lewan, M.D.; Stankiewicz, B.A. FTIR absorption indices for thermal maturity in comparison with vitrinite reflectance R0 in type-II kerogens from Devonian black shales. *Org. Geochem.* **2005**, *36*, 1533–1552. [CrossRef]

49.    Geng, W.; Nakajima, T.; Takanashi, H.; Ohki, A. Analysis of carboxyl group in coal and coal aromaticity by Fourier transform infrared (FT-IR) spectrometry. *Fuel* **2009**, *88*, 139–144. [CrossRef]

50.    Ibarra, J.; Munoz, E.; Moliner, R. FTIR study of the evolution of coal structure during the coalification process. *Org. Geochem.* **1996**, *24*, 725–735. [CrossRef]

51.    Chen, Y.; Mastalerz, M.; Schimmelmann, A. Characterization of chemical functional groups in macerals across different coal ranks via micro-FTIR spectroscopy. *Int. J. Coal Geol.* **2012**, *104*, 22–33. [CrossRef]

52.    Bushnev, D.A.; Burdel'naya, N.S. Khimicheskaya struktura kerogena i usloviya yego formirovaniya. *Geol. Geofiz.* **2009**, *50*, 822–829.

53.    Kawamura, K.; Tannenbaum, E.; Huizinga, B.J.; Kaplan, I.R. Long-chain carboxylic acids in pyrolysates of Green River kerogen. *Org. Geochem.* **1986**, *10*, 1059–1065. [CrossRef]

54.    Punanova, S.A. *Mikroelementy Neftej, Ich Ispol'zovanie pri Geochimičeskich Issledovanijach i Izucenii Processov Migracii*; Nedra: Moscow, Russia, 1974.

55. Xu, J.B.; Cheng, B.; Deng, Q.; Liang, Y.G.; Faboya, O.L.; Liao, Z.W. Distribution and geochemical significance of trace elements in shale rocks and their residual kerogens. *Acta Geochim.* **2018**, *37*, 886–900. [CrossRef]

56. Gottikh, R.P.; Pisotsky, B.I.; Plotnikova, I.N. Informativity of trace elements in the oil geology. *Georesursy* **2012**, *47*, 24–31.